

Anti-inflammatory and Anti-oxidative Effects of Some Medicinal Herbs on Chronic Murine Toxoplasmosis: A Histopathological and Immunohistochemical Study

Eman Mostafa Abd El-Rahman¹, Soad Mahdy Morsy Nada¹, Nagwa Ibrahim Hassan Ibrahim¹, Rasha Adel Attia², Shereen M. Ibrahim¹, Marwa Ahmed Salama¹

¹Medical Parasitology Department, Faculty of Medicine, Zagazig University, Zagazig, Egypt.

²Pharmacognosy Department, Faculty of Pharmacy, Zagazig University, Egypt.

Corresponding Author

Shereen M. Ibrahim

Mobile:

(+2) 01212756868

Email:

shery.redberry@gmail.com

© 2024 The author (s).
Published by Zagazig University. This is an open access article under the CC BY 4.0 license
<https://creativecommons.org/licenses/by/4.0/>

Receive date: 6/1/2024

Revise date: 26/2/2024

Accept date: 28/2/2024

Publish date: 2/3/2024

Keywords:

Toxoplasma gondii,
Lepidium sativum seed extract (LSSE), olive leaves extract (OLE), Resveratrol (RSV), Eucalyptus and Neuron Specific Enolase (NSE)

Background and study aim:

Toxoplasma gondii is a globally distributed parasite that causes oxidative stress as a part of the mechanism of neuropathology. The currently available treatments for toxoplasmosis are of limited efficacy because of its distinct pathophysiology. This study aimed to assess the anti-inflammatory and antioxidant effects of *Lepidium sativum* seed extract, olive leaves extract, resveratrol, and Eucalyptus either as a monotherapy or in combination with pyrimethamine-sulfadiazine in experimental toxoplasmosis by histopathological and immunohistochemical studies.

Patients and Methods: One-hundred-seventy-six Swiss albino mice were divided into eleven experimental groups (16 mice each) as follows Group (1) Control non-infected, Group (2) Control infected, Group (3) infected and treated with pyrimethamine-sulfadiazine, Group (4) infected and treated with RSV, Group (5) infected and treated with Eucalyptus,

Group (6) infected and treated with *Lepidium sativum*, Group(7) infected and treated with olives leaves extract, Group (8) infected and treated with pyrimethamine-sulfadiazine and RSV, Group(9) infected and treated with pyrimethamine-sulfadiazine and Eucalyptus, Group (10) infected and treated with pyrimethamine-sulfadiazine and *Lepidium sativum*, Group (11) infected and treated with pyrimethamine-sulfadiazine and olives leave extract.

Results: Histopathological examination of liver and brain tissues displayed marked improvement in all treated groups with a significant effect on the expression of iNOS and NSE, mainly in olives leaves extract treated groups.

Conclusion: Olive leaf extract, *Lepidium sativum* seed extract, resveratrol, and Eucalyptus can be promising efficient natural alternatives that can ameliorate the histopathological changes and oxidative stress triggered by the parasite during *Toxoplasma gondii* infection.

INTRODUCTION

Toxoplasma gondii (T. gondii) is a globally distributed protozoan parasite that infects about 30 to 50% of human populations [1]. The Centers for Disease Control have prioritized T. gondii as one of the top five neglected parasitic infections due to the severity of the illness it causes, high incidence, and low potential for prevention [2]. Oxidative stress (OS) occur when there is an imbalance between pro-oxidant

and antioxidant factors and is induced by reactive nitrogen species (RNS) and highly reactive oxygen species (ROS) [3]. ROS and RNS cause neuronal damage by inducing a negative effect on glial and neuronal cells. Neuronal cells are more susceptible to oxidative damage than other tissue cells. It is suggested that *Toxoplasma*-induced OS takes part in the mechanism of neuropathology and neurodegeneration [4].

Nitric oxide (NO) is a nitrogenous free radical secreted by a variety of mammalian cells. It has very important functions both in helminths and mammalian hosts as it promotes the cytotoxic and microbicidal activities of macrophages. The killer molecule NO is synthesized by inducible nitric oxide synthase (iNOS) [5]. Interestingly, it was found that in experimental Toxoplasmic Encephalitis (TE), iNOS is severely expressed in focal gliosis, microglia/macrophages, and in particular glial cells in the surrounding vasculature [6]. Moreover, it was mentioned that Neuron Specific Enolase (NSE) may be used as a marker to identify the severity of neuronal damage after cerebral ischemia [7]. Dincel and Atmaca mentioned that NSE expression contributes more to the interpretation of TE-related neuropathology [4].

Currently, toxoplasmosis is treated with sulfadiazine and pyrimethamine (PRY) [8]. Unfortunately, the drug resistance in *Toxoplasma gondii* that are resistant to the current drugs represents a concern both for treatment failure and for increased clinical severity especially in those of immunocompromised patients [9]. Medicinal plants have been recognized as potential drug candidates [10]. Herbal medicine or phytomedicine is the use of plants for medicinal and therapeutic purposes for curing diseases and improving human health. Plants have secondary metabolites called phytochemicals ('Phyto from Greek - meaning 'plant'). These compounds protect plants against microbial infections or infestations by pests. Phytochemicals are active ingredients which possess therapeutic properties [11].

Lepidium sativum is a popular herb that is commonly known in Arabic as (Hab el Rashaad or Thufa), grown in many regions of Saudi Arabia like Hijaz, the Eastern province, and Al-Qaseem [12]. It has an antiparasitic efficacy against *Eimeria tenella* [13], *Echinococcus granulosus* [14], and *T. spiralis* [15]. Many beneficial biological effects of *Eucalyptus* are known such as anti-oxidant activities, anti-microbial, anti-hyperglycemic, and anti-Trichomonas activity [16]. Its extracts contain cineol, terpenoids, and polyphenols that can display remarkable antioxidant activity [17]. It was also found that eucalyptol (the principal compound of the essential oils of *Eucalyptus* species) exhibits antioxidant activity because of the presence of phenolic compounds [18].

Maslinic acid (MA) (2R, 3-dihydroxyolean-12-en-28-oic acid) which is found in numerous plants is a triterpenoid compound related to oleanolic acid [19]. It is also found in considerable amounts, especially in fruit and leaves of *Olea europaea* (olives) [20]. Maslinic acid acts like other protease inhibitors by inhibiting intracellular replications and growth of *T. gondii* as well as blocking the parasite entry into the cell [21].

Resveratrol (trans-3,4',5-trihydroxystilbene, RSV), is a polyphenol found in many plants, especially peanuts, mulberries, and grapes [22]. It has a wide range of pharmacological activities, including antioxidant [23], anti-inflammatory [24], and anti-*T. gondii* [25]. Also, it helps in reducing oxidative stress contributes to prolonging the lifespan of organisms of different and also reduces the inflammation caused by the parasite [26]. We aimed in this research to assess the anti-inflammatory effects of medicinal herbs (*Lepidium sativum*, eucalyptus leaves extract, and olive leaves extract) and resveratrol against experimental *Toxoplasma gondii* infection in mice by histopathological and immunohistochemical study [5, 6].

PATIENTS/MATERIALS AND METHODS

Parasites and mice

Non-virulent ME49 strain of *T. gondii* was used for induction of chronic infection in mice. The strain was obtained from the Medical Parasitology Department at the Faculty of Medicine, Zagazig University in Egypt, maintained in the Animal House Center of the Faculty of Medicine at Zagazig University. Infected mice were sacrificed, and brains were removed under sterile conditions and homogenized with 1ml of normal saline, the number of tissue cysts was determined by placing 2 drops of each 20 μ l brain homogenate on slides and counted under light microscopy with magnifying (lens \times 40) and the count was multiplied by 20 to obtain the number of tissue cyst per brain [27]. 176 healthy laboratory-bred male Swiss albino mice weighing about 20-25gm each, aged 5 weeks was selected from the Animal House Center of the Faculty of Medicine, Zagazig University were conducted in this study.

Drugs and Plant material

Mice received pyrimethamine (12.5mg/kg) and

sulfadiazine (200mg/kg) (Sigma Aldrich). Their active ingredients were calculated for each mouse for every dose, and after that, its ingredients were dissolved in 0.5ml of 0.5% Tween-80 solution and given as a combination according to [28]. Resveratrol (100mg/kg) was purchased as a powder from (Sigma Aldrich). Its active ingredients were also calculated, and after that, its ingredients were dissolved in 0.5ml of 0.9% saline [29].

The fresh leaves of olive (*Olea europaea*) and Eucalyptus (*Eucalyptus Camaldulensis*) were collected from the experimental farm of the Pharmacognosy department, Faculty of Pharmacy, Zagazig University, Egypt. Dried seeds of cress (*Lepidium sativum*) were purchased from the local Egyptian market. The extract was prepared in the Pharmacognosy department, Faculty of Pharmacy, Zagazig University, Egypt. 500 g of fresh olive and Eucalyptus leaves and 300 g of dried cress seeds were cut into small pieces then, separately macerated into 80% methanol till complete exhaustion. The extracts were filtrated over filter paper and then the methanol was removed under reduced pressure at 50C to obtain semi-solid residues of crude plant extracts of 50 and 70 grams, respectively [30].

The suspensions of the dried extracts were prepared for oral administration using 0.5% Tween-80 (ADWIC, Egypt) as a suspending agent in normal saline. The concentration of each preparation was adjusted so that each 0.1 ml of the prepared suspension contains 1 mg of the plant extract, to achieve a dose of 200mg/kg for eucalyptus and olives leaves and *Lepidium sativum* seeds extract [31].

Experimental design

Mice were divided into eleven experimental groups (16 mice each) as follows Group (1) Control non-infected Group, (2) Control-infected non-treated, Group (3) infected and treated with pyrimethamine-sulfadiazine, Group (4) infected and treated with RSV, Group (5) infected and treated with Eucalyptus leaves extract, Group (6) infected and treated with *Lepidium sativum* seeds extract, Group (7) infected and treated with olives leaves extract, Group (8) infected and treated with both pyrimethamine-sulfadiazine and RSV, Group (9) infected and treated with both pyrimethamine-sulfadiazine and Eucalyptus leaves extract, Group (10) infected and treated with both pyrimethamine-sulfadiazine and

Lepidium sativum seeds, and Group (11) infected and treated with both pyrimethamine-sulfadiazine and olives leaves extract. All drugs and plant extracts were given once daily for 2 weeks, started 24 hrs. post-infection, orally as a liquid suspension by gavage.

Mice inoculation and scarification

Mice were orally infected with 10 cysts/ mouse using a 19-gauge gavage needle. Six weeks post-infection, mice were sacrificed, and their brain tissues were put in 10% formalin for both histopathology and immunohistochemistry studies.

Histopathology and immunohistochemistry (iNOs and NSE) Brain and liver tissues from the included groups were fixed in a 10% neutral buffered formalin solution. Paraffin blocks were prepared, sectioned between 3 and 5µm thickness then stained with hematoxylin and eosin for histopathological evaluation [32].

Other sections were prepared for immunostaining using Biotin-Streptavidin (BSA) [33]. To ensure proper deparaffinization, paraffin sections were put in Xylene overnight, and then these sections were brought to distilled water through 100%, 95%, 75%, and 50% ethanol. For antigen retrieval, Slides were placed in an unsealed plastic container filled with sufficient antigen retrieval solution (Citrate buffer solution, pH 6). The plastic container was placed in an open plastic tray to catch boil-over. Slides were put in a microwave oven (Samsung 800 Watts with digital control) at power 10 for 5 minutes. The amount of fluid in the container was checked and water was added if necessary to prevent slides from drying. Microwave for an additional 5 minutes on Power 10. The container was removed from the oven and allowed to cool for 15 minutes. Slides were then washed in deionized water several times then placed in phosphate buffer saline (PBS) for 5 minutes. Tissue sections were incubated with an endogenous peroxidase-blocking reagent containing hydrogen peroxide and sodium azide (DAKO peroxidase blocking reagent, Cat. No. S 2001). One to two drops of the supersensitive primary monoclonal antibody [against, Inducible nitric oxide synthase (iNOS, Cat. No. ABN26, Sigma-Aldrich) and Neuron-specific enolase (NSE, Cat. No. AB9698, Sigma-Aldrich) were then put on the sections. Slides were incubated horizontally in a humid chamber at room temperature for 60 min. After blotting off excess

buffer, 2 drops of DAKO EnVision + system were applied for 25 minutes at room temperature. Sections were then rinsed with PBS as before and blotted. Chromogen used was DAB (diaminobenzidine), 1-2 drops for 10-20 min. until a desirable brown color was obtained, the slides were then washed in the buffer. Sections were taken to distilled water then nuclear

counterstaining was done using Mayer's hematoxylin (Hx). Immunoreactive intensity was expressed by average grayscale. Values <160 were considered high, 160–170 medium, and 170–180 low [34].

RESULTS

Histopathological assessment

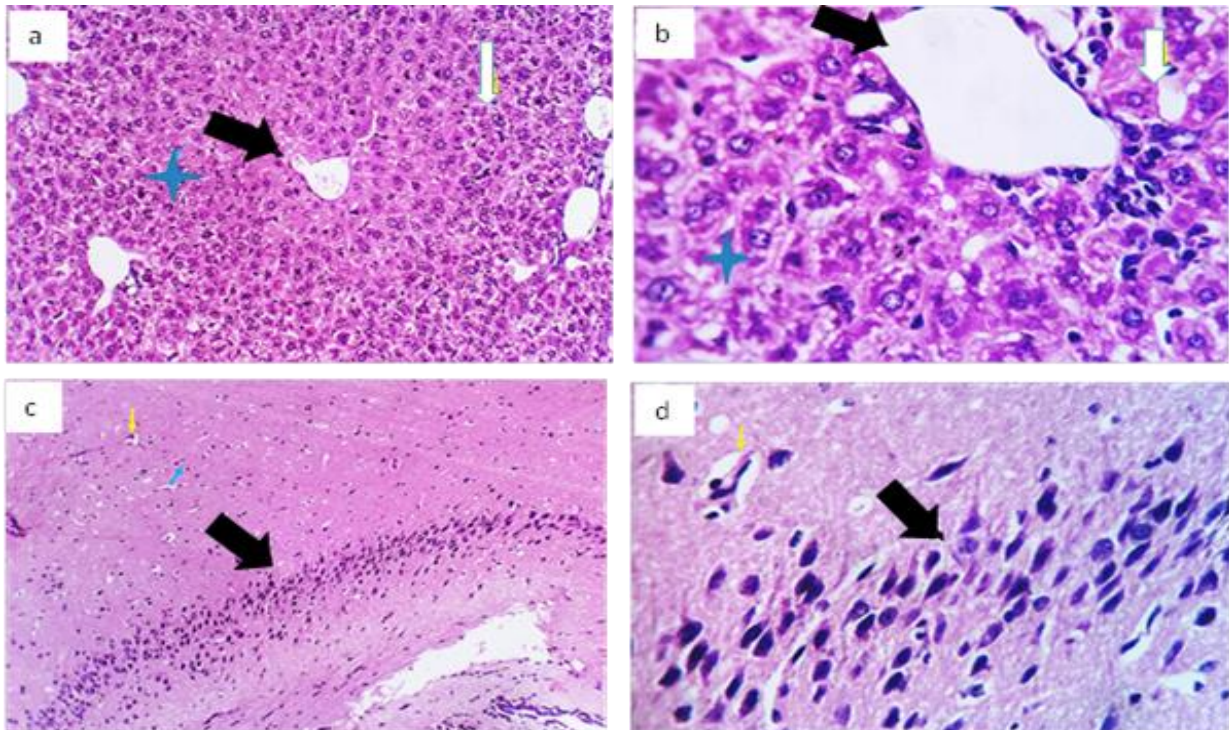


Figure 1. Photomicrographs from the liver (a, b) and brain (c,d) of G1 (non-infected and non-treated) showing normal hepatic parenchymal and stromal structures with preserved central veins (black arrows), portal triads (white arrow). Regarding cerebral and cerebellar cellular components, both showed normal histo-morphology with preserved cortical (blue arrow), blood vessels (yellow arrow), and hippocampus cellular components (black arrow) H&E X 100, 400.

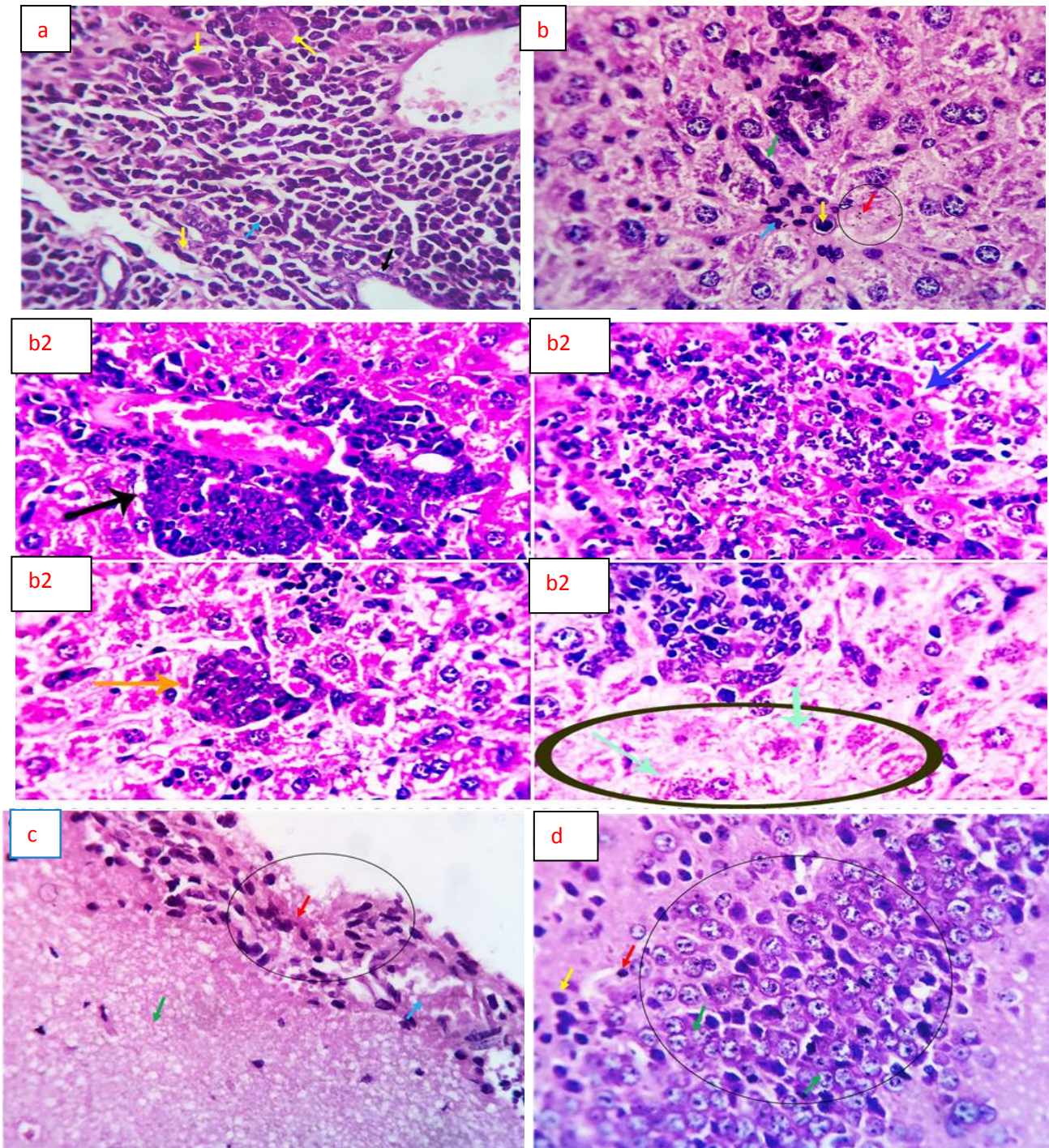


Figure 2 Photomicrograph from the liver (a, b, b2) of G2 (infected and non-treated) showing portal biliary reaction, lymphocytic cholangitis (thin black arrow), lympho-plasma-cytic infiltration (blue arrows), and individual cells apoptosis (red arrow), reticule-endothelial cells proliferation (green and thick black arrows). Some of the proliferating cells, mostly arise from hepatic satellite cells (HSCs), proliferative activities and abundant eosinophilic cytoplasm (yellow arrows) Vague parasitic cysts (b2 circle and light blue arrow), focal hepatocellular necrosis replaced by round cells (b2, blue arrow) and extra-medullary hematopoiesis (b2orange arrow). Photo-micrograph from the brain (c, d) showing meningoencephalitis with varying degrees of severity, the inflammatory cells consisted of lymphocytes, monocytes, macrophages, and occasional plasma cells in the meninges (circle, red and blue arrows), characteristic microglial/lymphocytic nodules with toxoplasmic - like material (maybe recently ruptured cysts) in the hippocampal tissue (red and yellow arrows) and a specific focal neuronal cells proliferation (circle and green arrows) H&E X 200, 400.

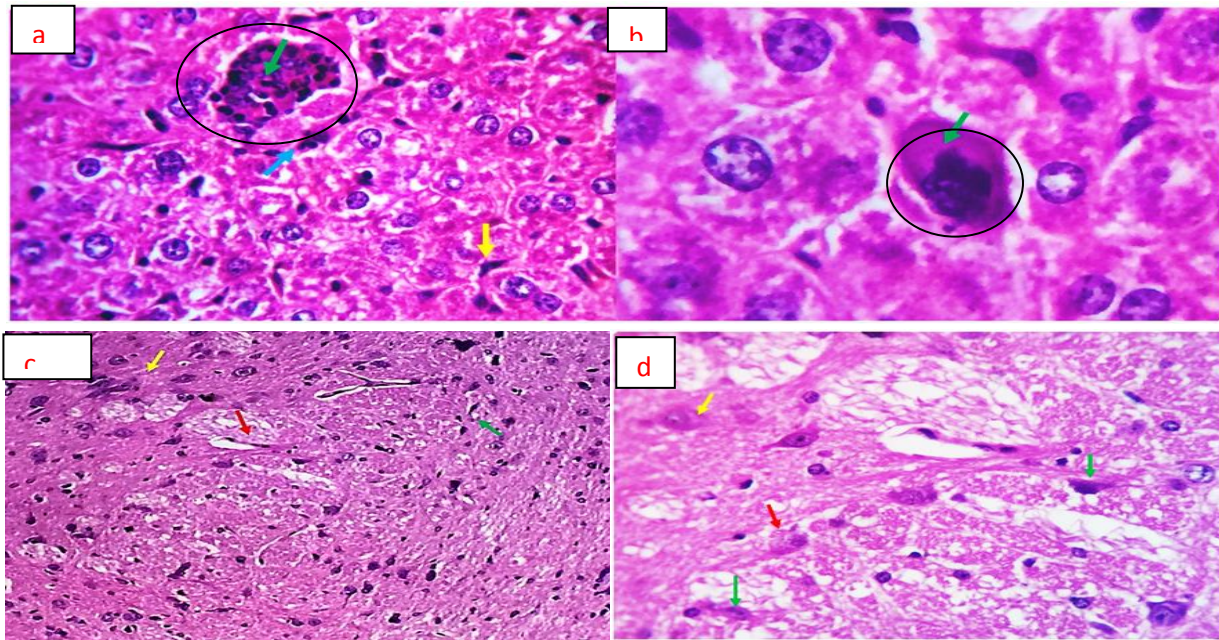


Figure. 3 Photo-micrograph from the liver (a, b) of G3 (infected and treated with PYR and SDZ) showing that marked extramedullary erythropoiesis with multiple distributed lymphoid, myeloid and megakaryocytic cells (green arrows, blue arrow, and circles). The Von Kupffer cells were hypertrophied (yellow arrow). Photo-micrograph from the brain (c,d) showing focal neuronal (yellow arrow) and axonal degeneration (red arrow) with reactive astrocytosis (green arrow) H&E X 200, 400.

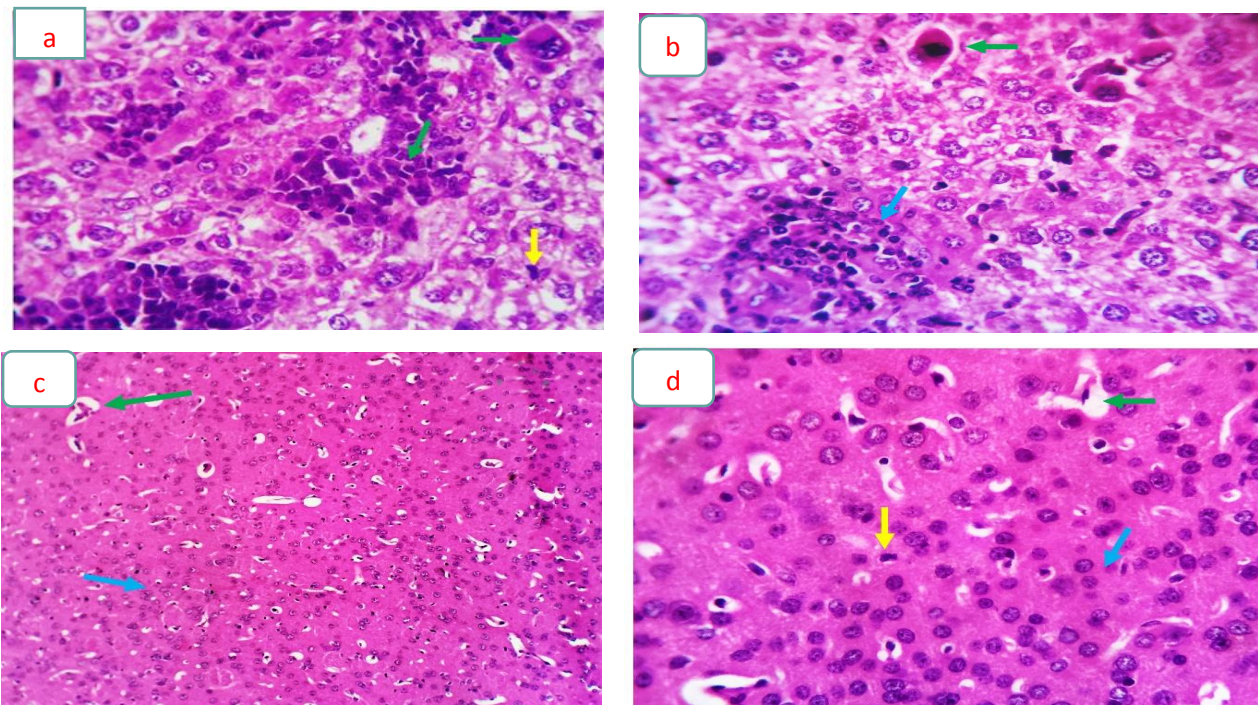


Figure 4 Photo-micrograph from the liver (a, b) of G4 (infected and treated with RSV) showing normal parenchymal and portal histo-morphological structures. Characteristic extramedullary erythropoiesis with multiple distributed lymphoid, myeloid, and megakaryocytic cells in the hepatic interstitial tissue (green arrows), residual focal necrotic areas partially replaced by round cells, and aggregated proliferated endothelial cells (endotheliosis) (blue arrow) and the Von Kupffer cells were hypertrophied (yellow arrow). Photomicrograph from brain (c, d) showing normal structural configurations including, cerebral cortical cells (blue arrow), neuropils, glial cells (yellow arrow), and vascular structures (green arrow) H&E X 200, 400.

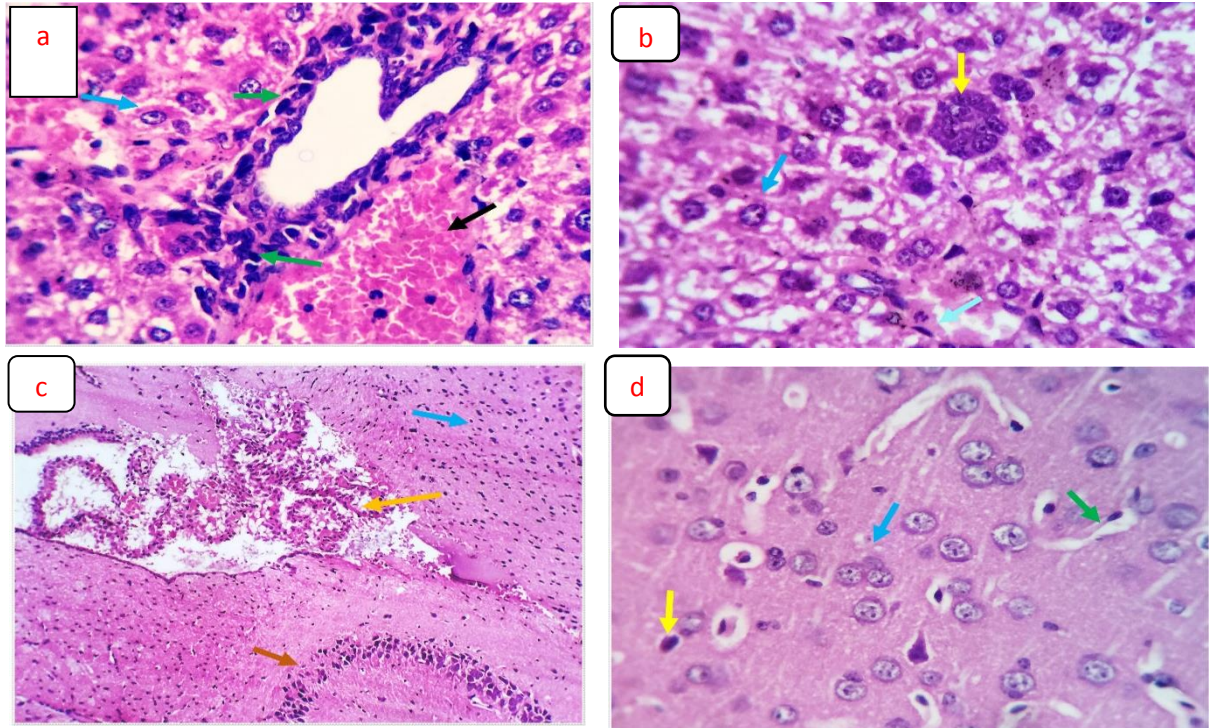


Figure 5 Photo-micrograph from the liver (a, b) of G5 (infected and treated with *Eucalyptus* leaves extract) showing normal parenchymal cells (blue arrows). Moderate portal vascular congestion (black arrow), lymph-plasmacytic infiltration (green arrows), and interstitial aggregates of proliferated endothelial cells (endotheliosis) (yellow arrow) and the Von Kupffer cells were apparently (light blue arrow). Photo-micrograph from the brain (c, d) normal structural configurations of cerebral vascular structures (green arrow), cortical cells (blue arrow), hippocampal cells (brown arrow), neuropils and glial cells (yellow arrow), and lateral ventricular choroid plexus hyperplastic change was seen (orange arrow) H&E X 200, 400.

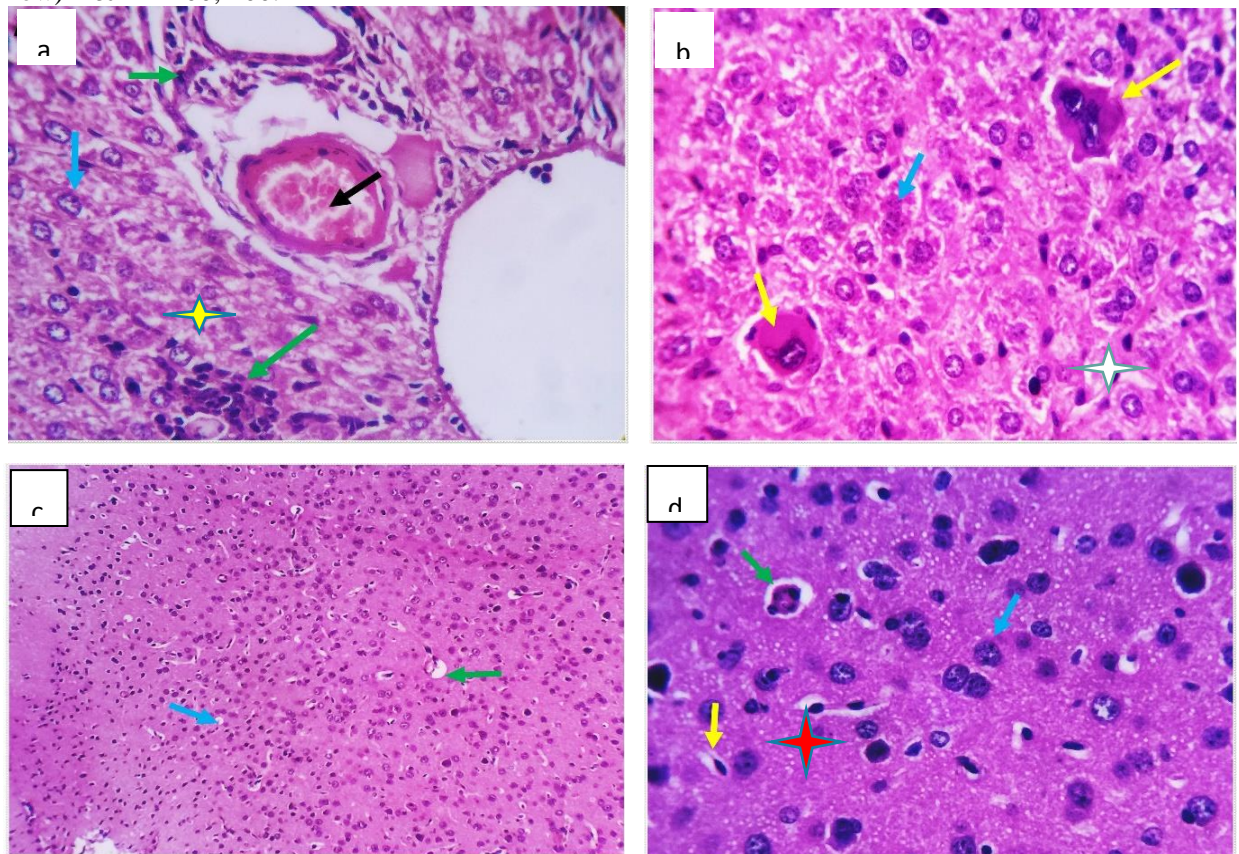


Figure 6 Photo-micrograph from the liver (a, b) of G6 (infected and treated with LSSE) showing normal parenchymal and portal histo-morphological structures. Mild portal vascular congestion (black arrow), edema (yellow star), and round cell infiltration (blue arrow). The latter is also seen in the interstitial tissue (green arrow), typical mono or multi-nuclear pleomorphic cells with abundant eosinophilic cytoplasm (yellow arrows), and Von Kupffer cells were hypertrophied (white star). Photo-micrograph from the brain (c, d) showing normal structural configurations concerning the meninges, vascular structures (green arrows), cerebral cortical cells (blue arrows), neuropils and glial cells (yellow arrow), and few cortical neuronal cells appear pyknotic (red stars) H&E X 200, 400.

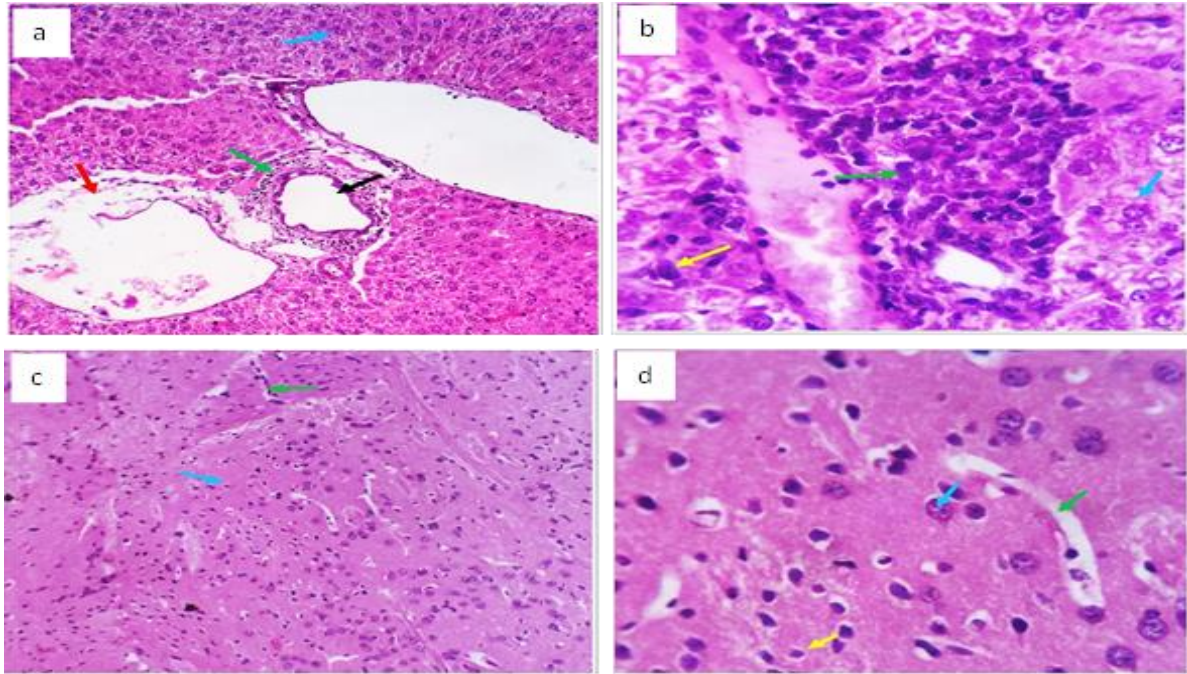


Figure. 7 Photo-micrograph from the liver (a, b) of G7 (infected and treated with Olives leaves extract) showing normal hepatocytes (blue arrow), mild portal biliary proliferation (black arrow) vascular congestion, edema (red arrow) and round cells aggregation (green arrow) and Von Kupffer cells were hypertrophied (yellow arrow). Photo-micrograph from the brain (c, d) showing normal structural configurations concerning the meninges, vascular structures (green arrows), cerebral cortical cells (blue arrows), and neuropils and glial cells (yellow arrow) H&E X 200, 400.

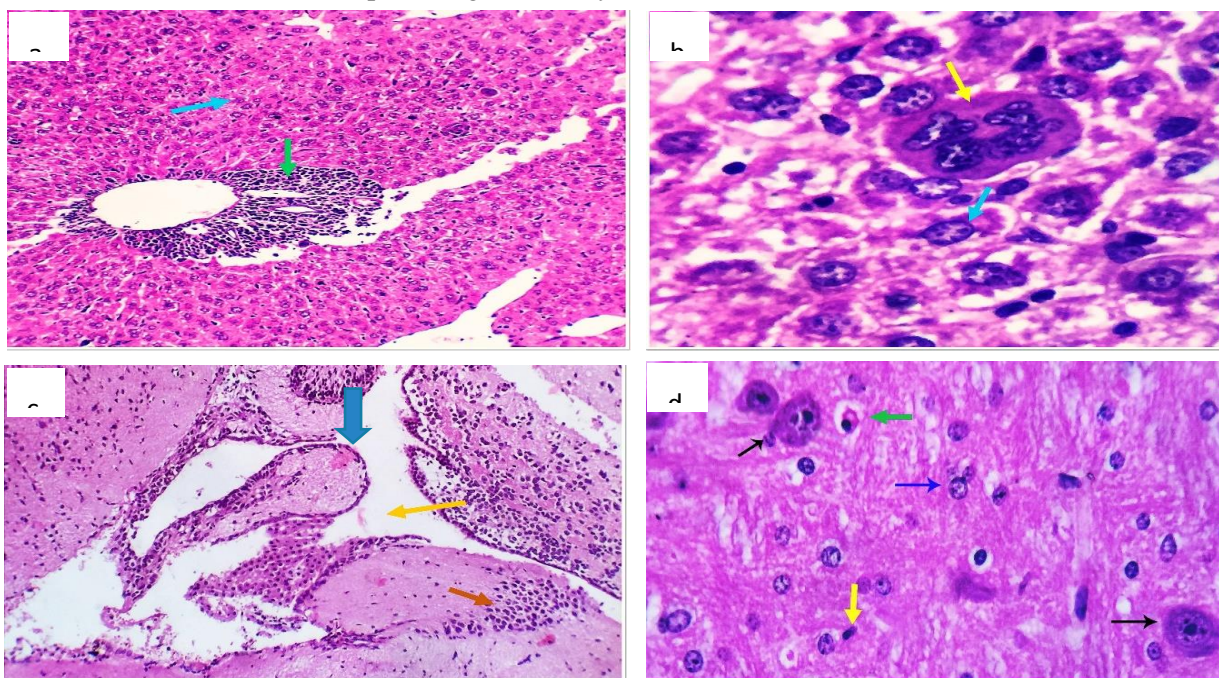


Figure 8. Photo-micrograph from the liver (a, b) of G8 (infected and treated with combined PYR-SDZ with RSV) showing normal hepatocytes (blue arrow), mild portal biliary proliferation, and moderate round cells aggregation (green arrow) and typical mono or multi-nuclear pleomorphic cells with abundant eosinophilic cytoplasm (yellow arrow). Photo-micrographs from the brain (c, d) showing normal structural configurations concerning vascular structures (green arrow), cerebral cortical cells (blue arrow), neuropils and glial cells (yellow arrow), mild edema and choroid plexus proliferative changes were recorded in the lateral ventricle (orange arrow), few cortical neuronal cells degeneration (black arrows) and focal microgliosis (red arrow). H&E X 200, 400.

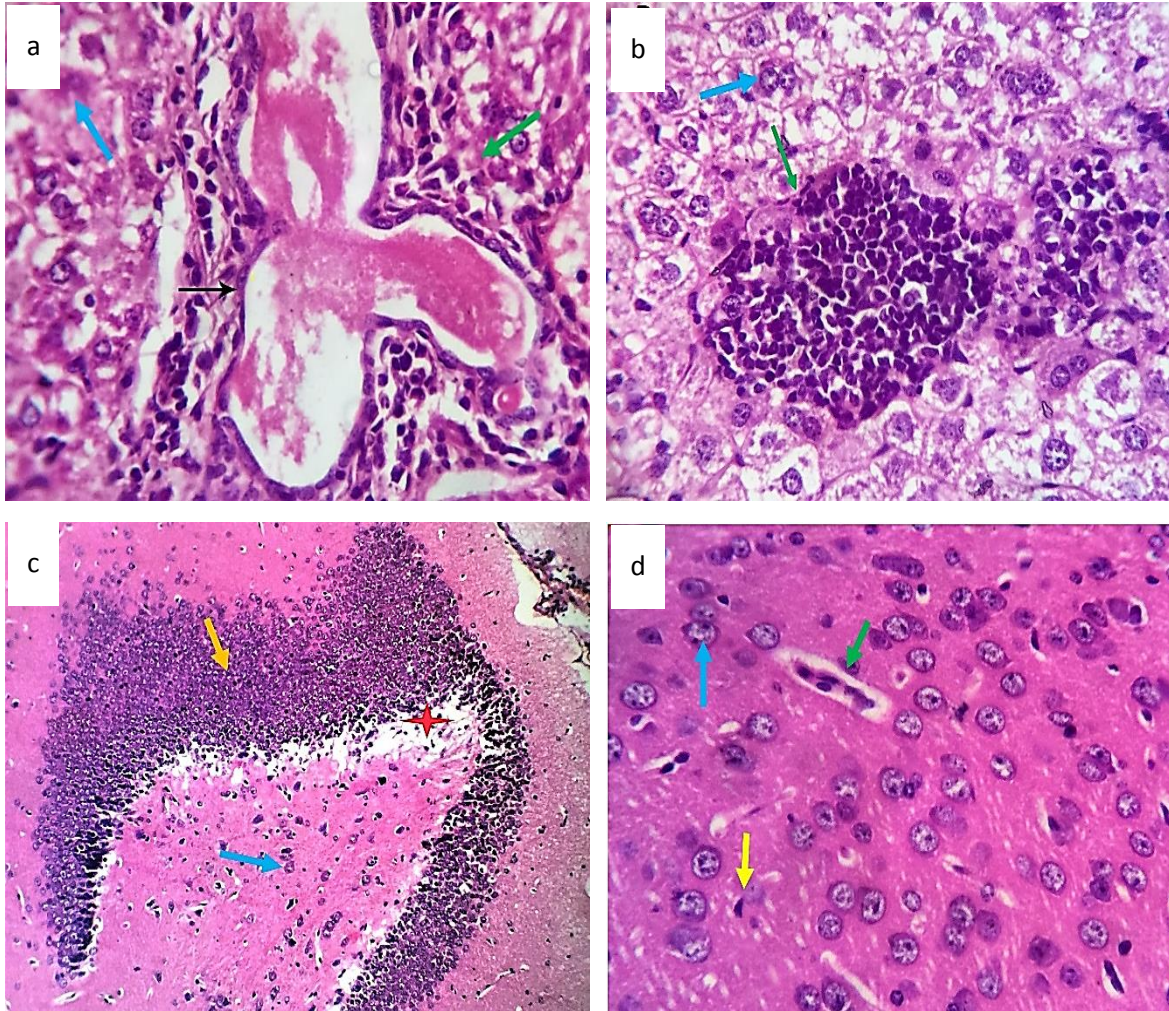


Fig 9 Photo-micrograph from the liver (a, b) of G9 (infected and treated with combined PYR-SDZ with *Eucalyptus*) showing normal parenchymal and portal histomorphological structures. Mild biliary proliferation with cystification with portal interstitial lymphoplasmacytic aggregations (black and green arrows) and focal mild degenerated hepatocytes (blue arrow). Photomicrograph from the brain (c, d) showing normal structural configurations concerning, vascular structures (green arrow), cerebral cortical cells (blue arrow), neuropils and glial cells (yellow arrow), characteristic hippocampal granular cell proliferation (orange arrow) and focal neuropil demyelination (red star). H&E X 200, 400.

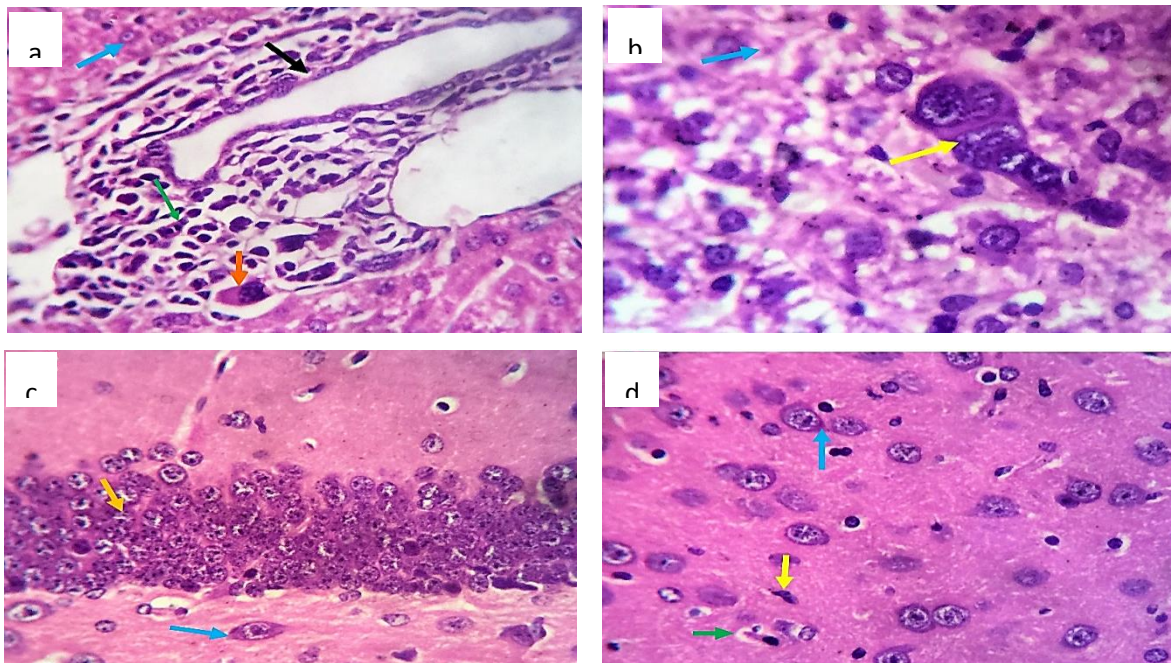


Figure. 10 Photo-micrograph from the liver (a, b) of G10 (infected and treated with combined PYR-SDZ with LSSE) showing normal parenchymal and portal micro-morphological structures. Hepato-portal biliary proliferation with cystification and round cell aggregations (black and green arrows) and focal mild degenerated hepatocytes (blue arrow). Marked reticuloendotheliosis (yellow arrow) and focal megakaryocytosis (orange arrow). Photo-micrograph from the brain (c, d) showing normal structural configurations including vascular structures (green arrow), cerebral cortical cells (blue arrow), neuropils and glial cells (yellow arrow), and mildly proliferated hippocampus cells (orange arrow). H&E X 200, 400.

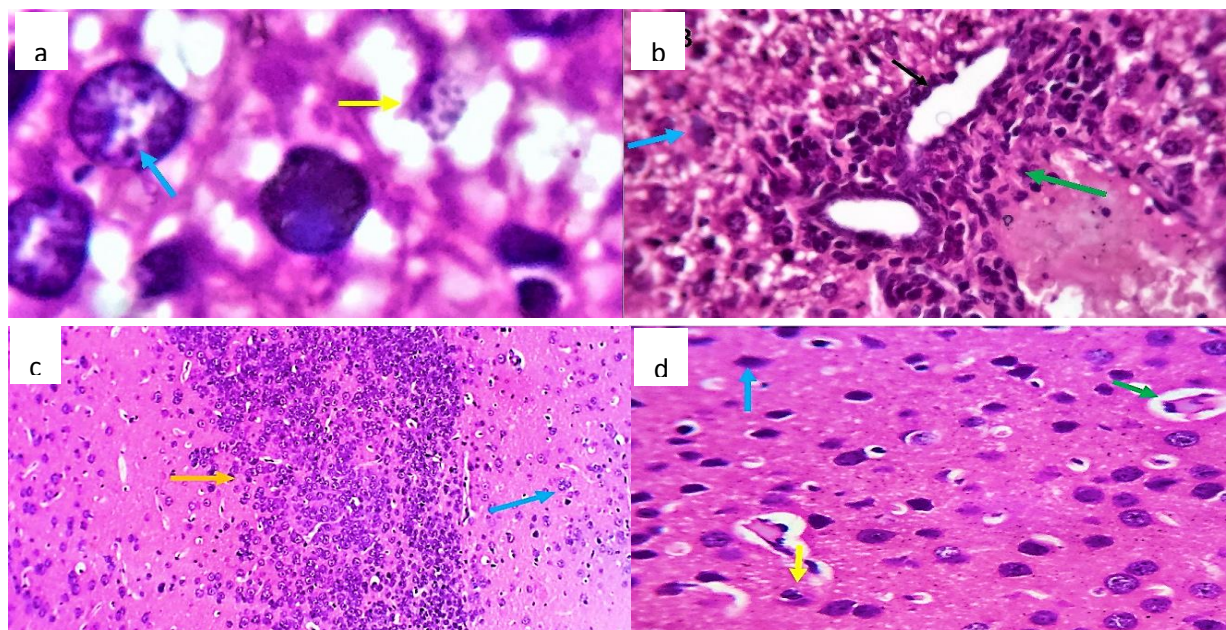


Figure. 11 Photo-micrograph from the liver (a, b) of G11 (infected and treated with combined PYR-SDZ with Olive leaves extract) showing mild hepatoportal biliary proliferation and round cells aggregations (green arrow), few hepatocytes with marginated chromatin (blue arrow), extra and intracellular amorphous rounded structures of unspecific nature which may be degenerated protozoans (yellow arrow). Photo-micrograph from the brain (c, d) showing normal structural configurations including vascular structures (green arrow), cerebral cortical cells (blue arrow), neuropils, and glial cells (yellow arrow). Focal oligo-dendrogliosis (orange arrow) H&E X 200, 400.

Abd El-Rahman et al., Afro-Egypt J Infect Endem Dis, March 2024;14(1):94-112

<https://aeji.journals.ekb.eg/>

DOI: 10.21608/AEJI.2024.258749.1346

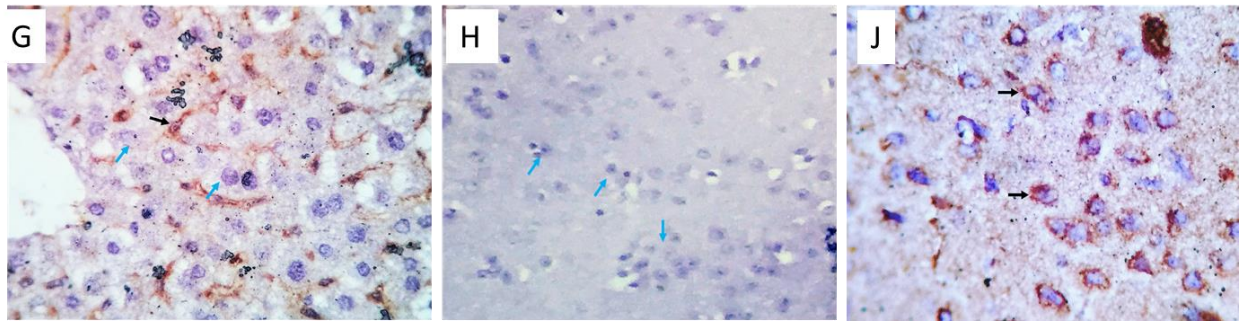
Immunohistochemical assessment:

Figure. 12 Photo-micrographs from the liver (G) and brain (H, J) of G1 showing negative expression of iNOS in examined tissues however, positively reactive hepatic Von Kupffer cells and stromal lymphoid cells (blue and black arrows G). NSE immunostaining declared a moderately positive (brownish cytoplasmic stainability) staining reaction in different parts of cerebral and cerebellar cellular components (blue and black arrows H, J). X 400.

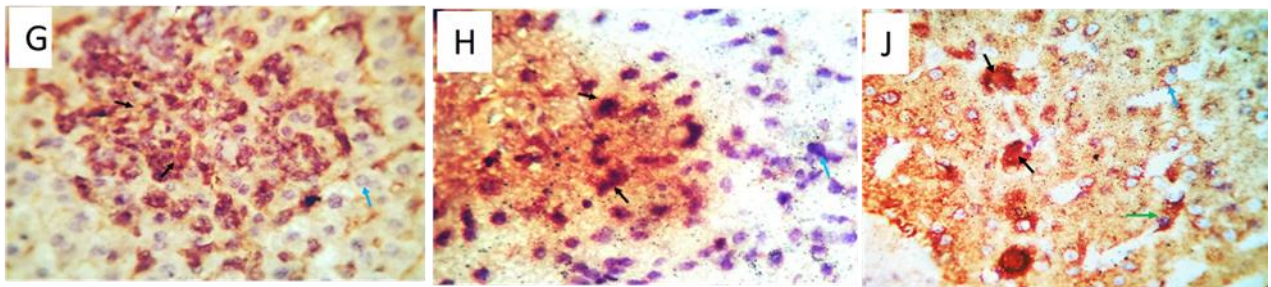


Figure. 13 Photo-micrographs from the liver (G) and brain (H, J) of G2 showing strong positive iNOS expression in hepatic Von Kupffer (G, blue arrows), inflammatory cells (G, black arrows) and degenerated neurons (H, black arrows). a strong positive NSE immunostaining (brownish cytoplasmic stainability) in some degenerated neuronal cells (J, black arrows) and in reactive glial cells (J, green arrows), and a weak non-specific reaction was seen in normal neurons (blue arrows) X200, 400.

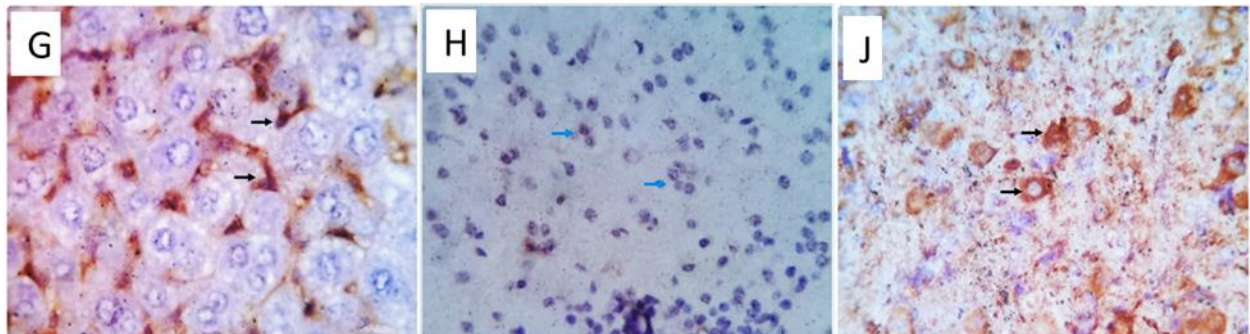


Figure. 14 Photo-micrographs from the liver (G) and brain (H, J) of G3 showing some of the hepatic Von Kupffer cells were moderately stained against iNOS specific antibodies (black arrows), positive reaction to NSE was seen in some of the degenerated cerebral cells (black arrow), other cerebral cells were non-specifically reacted to the used marker negatively stained cells (blue arrow) X200, 400.

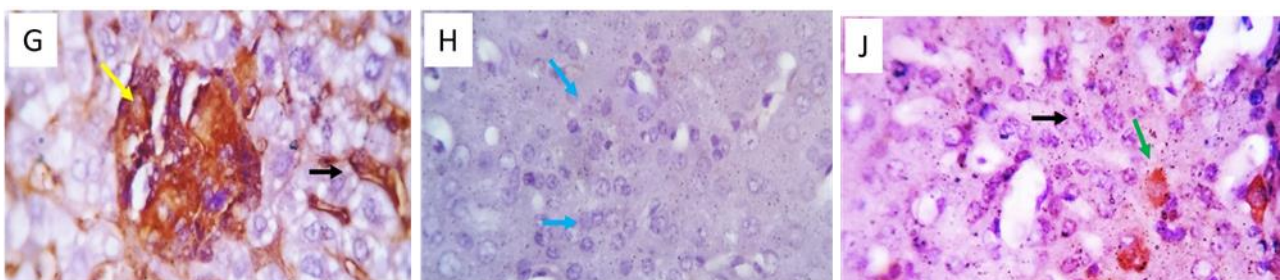


Figure 15 Photo-micrographs from the liver (G) and brain (H, J) of G4 showing negative expression of iNOS and NSE in different tissue sections. Some round cell aggregates (endotheliosis or hematopoietic cells) and Von Kupffer cells were mildly to moderately stained against iNOS (yellow and black arrows). Positive reaction to NSE in degenerated cerebral cells (green arrow, J) and other cerebral cells (black arrow, J) negatively stained cells (blue arrow H) X200, 400.

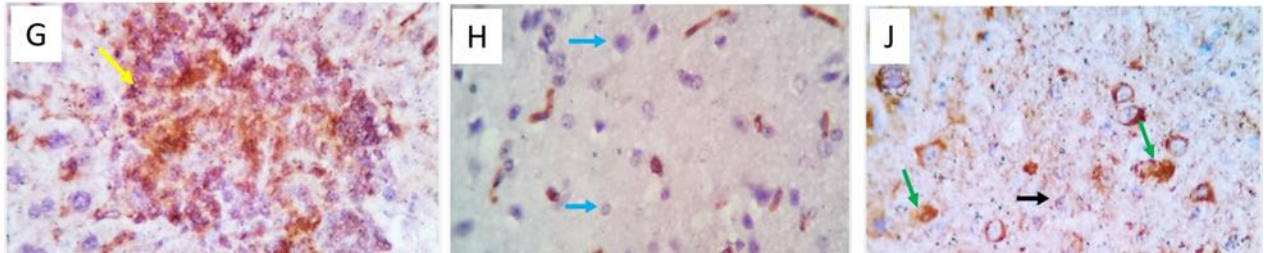


Figure.16 Photo-micrographs from the liver (G) and brain (H, J) of G5 showing negative expression of the used markers in different tissue (blue arrows), some of the hepatic round cell aggregates (focal endotheliosis or hematopoietic cells) are mildly to moderately stained against iNOS specific antibodies (yellow arrow). Positive reaction to NSE was seen in a few degenerated cerebral cells (green arrows), other cerebral cells were negatively stained (black arrow) X 400.

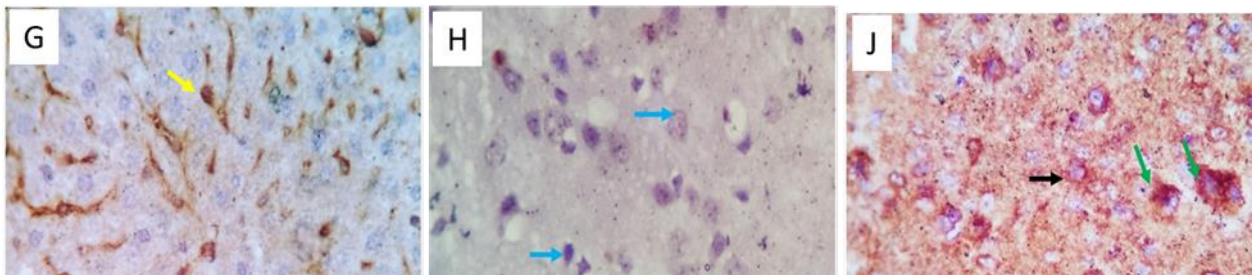


Figure. 17 Photo-micrographs from the liver (G) and brain (H, J) of G6 showing negative expression of the used markers in different tissue (blue arrows), some of the hepatic Von Kupffer cells appear mildly stained against iNOS specific antibodies (yellow arrow). positive reaction to NSE was seen in some degenerated cerebral cells (green arrows), other cerebral cells appear unspecifically stained (black arrow) X 400.

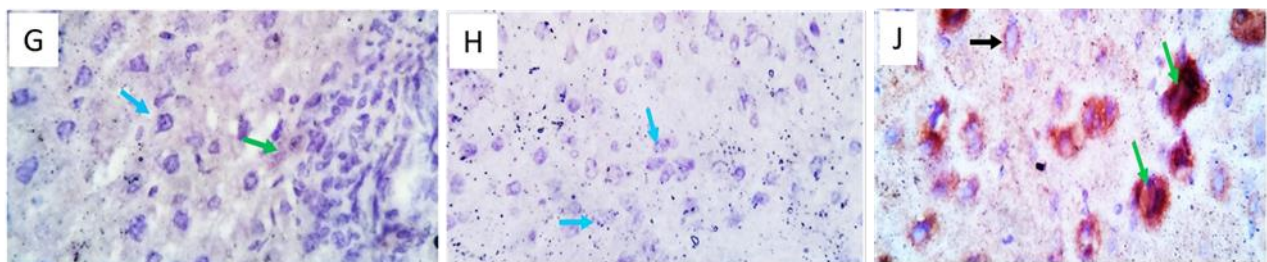


Figure. 18 Photo-micrographs from the liver (G) and brain (H, J) of G7 showing negative expression of the used markers in different tissue (blue arrows) and some of the hepatic Von Kupffer cells were mildly stained against iNOS specific antibodies (green arrow). positive reaction to NSE was seen in some of the degenerated cerebral cortical cells (green arrows), other cerebral cells appear unspecifically stained (black arrow) X 400.

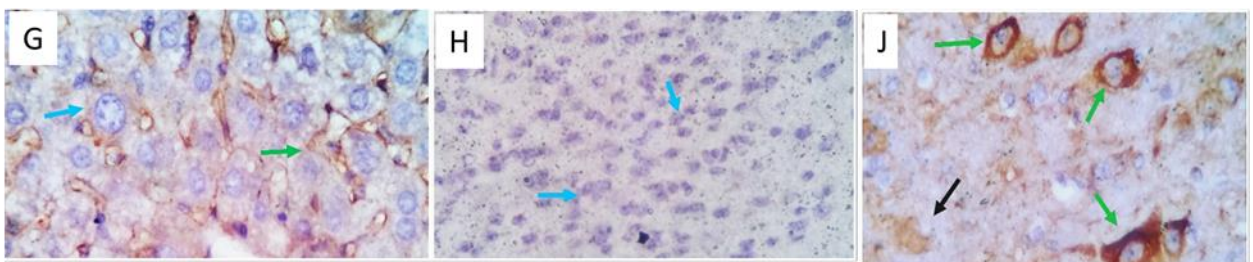


Figure. 19 Photo-micrographs from the liver (G) and brain (H, J) of G8 showing negative expression of the used markers in different tissue (blue arrows), some of the hepatic Von Kupffer cells appear mildly stained against iNOS specific antibodies (green arrow). positive reaction to NSE in some degenerated cerebral cortical cells (green arrows), other cerebral cells appear unspecifically stained (black arrow) X 400.

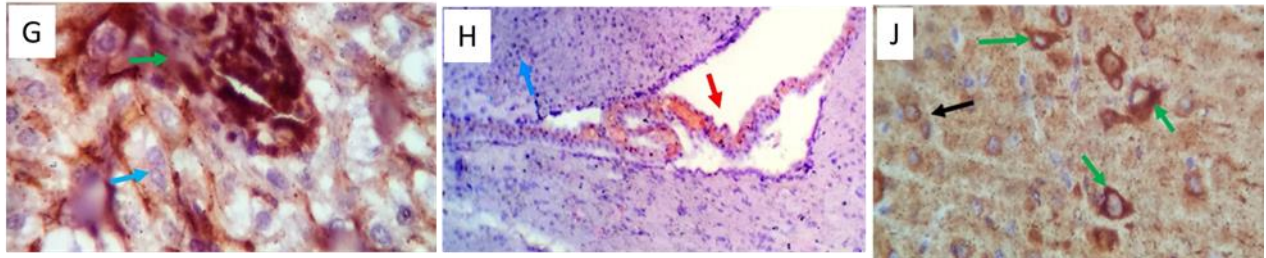


Figure. 20 Photo-micrographs from the liver (G) and brain (H, J) of G9 showing negative expression of the used markers in different tissue (blue arrows), normal brain choroid plexus was positively reacted (red arrow). Focally aggregated hepatic lymphoplasmacytic cells appear mildly stained against iNOS-specific antibodies (green arrow). Positive reaction to NSE in some degenerated cerebral cortical cells (green arrows), other cerebral cells were unspecifically stained (black arrow) 200, X 400.

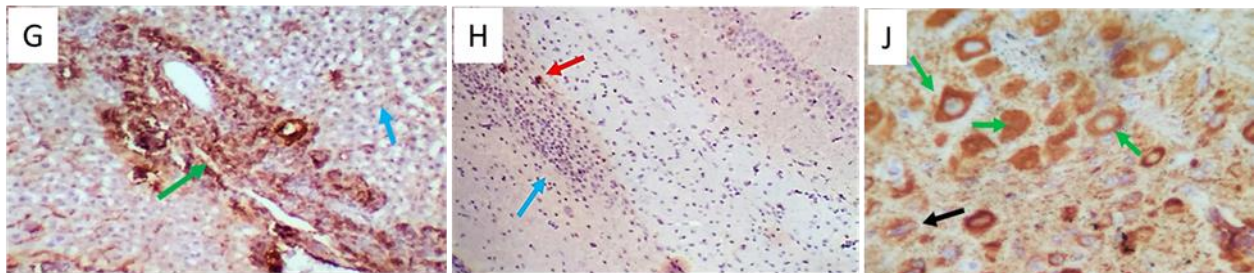


Figure. 21 Photo-micrographs from the liver (G) and brain (H, J) of G10 showing negative expression of the used markers in different tissue (blue arrows), hepato-portal aggregated lymphoplasmacytic cells are moderately reacted against iNOS specific antibody (green arrow), very few degenerated cerebral cortical cells were mildly stained to iNOS (red arrow). positive reaction to NSE in some of the degenerated cerebral cortical cells (green arrows), other cerebral cells were unspecifically stained (black arrow) X100, 400.

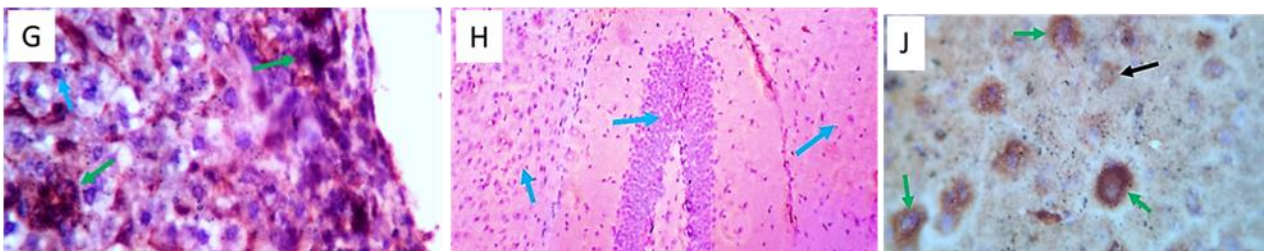


Figure. 22 Photo-micrographs from the liver (G) and brain (H, J) of G11 showing negative expression of the used markers in different tissue (blue arrows), hepato-portal aggregated lymphoplasmacytic cells, and interstitial reticuloendothelial cells are mildly reacted to iNOS specific antibody (green arrow). Positive reaction to NSE in some of the degenerated cerebral cortical cells (green arrows), other cerebral cells were unspecifically stained (black arrow) X100, 400.

Morphometric analysis

Regarding the immunohistochemical finding, a significant decrease in iNOS expression in both liver and brain tissues and NSE in brain tissues was observed in all treated groups in comparison with infected non-treated ones. The marked decline was observed in OLE-treated groups (G7 and G11). The mean expression of iNOS in the liver and brain in G7 was (5.6 and 2.6) respectively. While the mean expression of NSE is 8.8. Furthermore, the mean expression of iNOS in the liver and brain in G11 was (4.9 and 2) respectively. The least expression of NSE was seen in G11 (7.3), $p < 0.001$ (Table 1).

Table 1: The mean expression of INOS (liver and brain) and NSE (brain)

Groups	INOS in liver	INOS in brain	NSE in brain
	Mean \pm SD	Mean \pm SD	Mean \pm SD
G1	2.41 \pm 1.00 ^d	2.44 \pm 0.58 ^d	4.04 \pm 1.64 ^c
G2	<u>23.12\pm 5.85^a</u>	<u>22.14\pm3.18^a</u>	<u>87.02\pm9.40^a</u>
G3	12.18 \pm 2.69 ^c	9.96 \pm 2.01 ^b	35.02 \pm 4.58 ^b
G4	12.08 \pm 2.18 ^c	5.24 \pm 2.40 ^c	18.28 \pm 6.38 ^c
G5	12.82 \pm 1.16 ^c	4.06 \pm 1.84 ^{c,d}	11.28 \pm 3.85 ^{d,e}
G6	12.86 \pm 1.85 ^c	3.18 \pm 1.76 ^{c,d}	13.94 \pm 2.87 ^{c,d}
G7	5.62 \pm 2.44 ^d	2.62 \pm 1.17 ^d	8.84 \pm 3.62 ^{d,e}
G8	7.84 \pm 1.42 ^d	3.80 \pm 1.99 ^{c,d}	13.62 \pm 1.93 ^{c,d}
G9	12.82 \pm 2.48 ^c	3.66 \pm 1.54 ^{c,d}	14.26 \pm 5.20 ^{c,d}
G10	16.80 \pm 4.02 ^b	3.98 \pm 1.00 ^{c,d}	13.80 \pm 3.01 ^{c,d}
G11	4.92 \pm 0.96 ^d	2.02 \pm 0.64 ^d	7.32 \pm 1.08 ^c
F-test	22.623	52.478	131.203
P-value	<0.001**		

There is no significant difference between any two groups, within the same column that has the same superscript letter, **Mean \pm SD**: Mean \pm standard deviation **F**: ANOVA test, **P**: Probability, **: Highly significant difference.

DISCUSSION

Drug therapy for *T. gondii* is difficult because of its distinct pathophysiology [31]. To cause a persistent infection, the parasite penetrates the blood-brain barrier [35]. Treatment of persistent infection is challenging because the blood-brain barrier prevents the transfer of appropriate medication concentration [36].

There are few effective treatments for toxoplasmosis at the moment, and many of them

have negative side effects. Therefore, it is essential to look for substitute chemicals with new modes of action [37]. In comparison to the current anti-toxoplasma medicines, natural chemicals, and traditional herbal medicine are highly available and have fewer adverse effects [38]. From our previous work, we found that natural plants (*Lepidium sativum*, *Eucalyptus*, and Olive leaf extract) and resveratrol showed anti-toxoplasma effect via significant reduction of the brain cysts count when used either as

monotherapy or combined with PYR and SDZ (unpublished data). In the current investigation, we sought to assess the anti-inflammatory effects of OLE, LSSE, Eucalyptus, and RSV against chronic experimental *T. gondii* infection in mice. Drugs were used separately as well as in conjunction with PYR and SDZ. Analysis using, histopathological and immunohistochemical methods was used to evaluate the situation.

Regarding the histopathological and immunohistochemical finding, our results showed that G2 (infected non-treated group) had strong positive iNOS expression in hepatic Von Kupffer, inflammatory cells, and degenerated neurons. Further, a strong positive NSE immunostaining appeared as brownish cytoplasmic stainability in some degenerated neuronal cells and reactive glial cells. On the same side, Mahmoudvand et al. demonstrated that mRNA levels of iNOS significantly increased in chronic *T. gondii* infection [39]. They added that chronic *T. gondii* infection communication among immune cells promotes neuroinflammation through cytokine networks and induces pathological progression of Alzheimer's disease (AD) in the mice brain. Furthermore, Dincel and Atmaca showed a statistically significant increase in the expression of NSE, confirming the severity of degeneration in the CNS in TE [4]. They added that oxidative stress and expression of NSE might give an idea of the disease progress and may also have a critical diagnostic significance for patients infected with *T. gondii*.

We observed an improvement in the histopathological appearance of liver and brain tissue evidenced by a decrease in inflammatory cells and an improvement in the tissue structure towards the normal, also, there was a decrease in iNOS level in the liver and brain, and NSE level in the brain detected by both photo-micrographs and morphometric analysis. The greatest improvement was found in OLE-treated groups. We proposed that this effect was attributed to the anti-inflammatory effect of the MA and oleuropein. According to Omar the anti-inflammatory effect of oleuropein was related to the reduction of lipoxygenase activity and the formation of leukotriene B4 [40].

This agreed with Abugomaa and Elbadawy who observed that OLE improved the histological appearance of renal glomeruli and renal tubules as well as retained the normal histological

appearance of hepatic lobules in glycerol-exposed rats [41].

In LSSE-treated groups, the improvement in the histopathological and immunohistochemical findings of liver and brain tissue can be due to its anti-inflammatory and antioxidant activities. The primary component of *L. sativum* seeds is -linolenic acid, which suppresses the expression of iNOS and prevents NO generation. According to Ren and Chung linolenic acid may exert this action by preventing NF- κ B activity and the phosphorylation of mitogen-activated protein kinase (MAPK) in macrophages [42].

The ethanolic extract of *L. sativum* significantly decreased iNOS-2 expression and nitrate concentration. Nuclear factor kappa-B (NF- κ B) nuclear expression, NF- κ B DNA binding activity, and cytokines (TNF- and IL-6) were all considerably downregulated by the reduction in nitrosative stress in a dose-dependent manner [43]. This agreed with Al-Otaibi et al. who observed that LSSE improved histopathological changes in the liver of *Trypanosoma evansi*-infected mice [44], also, with Balgoon who observed that LSSE restored the normal hepatic and renal structure in rats exposed to aluminum-induced hepatic and renal toxicity [45]. As regards Eucalyptus extract treated groups, the obtained results may be attributed to the antioxidant and the anti-inflammatory potential of Eucalyptus extract and inhibition of TNF α , IL6, NO, iNOS, and COX-2 expression. This agreed with Mousa et al. who detected that Eucalyptus attenuated diclofenac sodium-induced pathological alterations in hepatic tissues of rats [46].

In RSV-treated groups, we proposed that the anti-inflammatory effect of RSV is due to the antioxidant properties of this compound and its ability to decrease IL1 β . RSV decreased the generation of NO in the macrophages of mice with *Leishmania* infection, according to Mousavi et al [47]. This agreed with Highab et al. who detected that RSV reduced the hepatocytes injury and preserved the liver parenchyma in rats exposed to lead intoxication [48]. It has been proven that *T. gondii* elicits robust innate and TH1 adaptive immune responses in the CNS, where the expression of inflammatory cytokines and mediators such as NO has both protective and pathological effects [49]. Although these factors restrict parasite replication and spread, inflammatory responses can also cause

considerable injury to uninfected neurons and can additionally influence neurotransmitter functions and synaptic transmission [50].

CONCLUSION

In conclusion, there was a great improvement in the histological appearance of the liver and brain in all treated groups compared to the control group (G2). All treated groups showed a significant effect on the expression of iNOS and NSE in both liver and brain mainly OIE treated groups (7 and 11). In addition, the medicinal plants (OLE, LSSE, Eucalyptus) and RSV could be an efficient alternative to traditional treatment of *Toxoplasma gondii* by ameliorating the histopathological changes that were caused by toxoplasmosis.

Funding: This research did not receive any specific grant from funding agencies in the public, commercial, or not-for-profit sectors.

Conflict of Interest: None.

Ethical considerations:

Mice were reared and sacrificed according to the protocol of The Institutional Animal Care and Use Committee of Zagazig University (ZU-IACUC) for Animal Use in Research and Teaching. All procedures were done under anesthesia and all efforts were made to ensure minimal animal suffering. As *T. gondii* is a bio-safety level 2(BI-2) pathogen, appropriate precautions were followed when handling the parasite. Care was taken to avoid infection of assisting personnel during the parasite-animal passage. The study protocol was approved by the Medical Parasitology Department Review Board (Approval No, ZU-IACUC/3/F/95/2020).

HIGHLIGHTS

- *Toxoplasma gondii* (*T. gondii*) is a globally distributed parasite that was prioritized as one of the top “Five Neglected Parasitic Infections.”
- There are few effective treatments for toxoplasmosis at the moment, because of its distinct pathophysiology as the parasite penetrates the blood-brain barrier and this makes treatment of persistent infection challenging .
- Herbal medicine or phytomedicine is the use of plants for curing diseases and improving human health .
- Anti-toxoplasma medicinal plants (OLE, LSSE, Eucalyptus and RSV) which were

highly available an efficient alternative to the traditional treatment of *Toxoplasma gondii*.

- Neuron Specific Enolase (NSE) marker expression was a good assessment tool to measure the antioxidant effect of the used medicinal plants against experimental toxoplasmosis .

REFERENCES

1. World Health Organization (WHO). Toxoplasmosis Fact Sheet. World Health Organization: Geneva 2015. Available at: https://www.euro.who.int/__data/assets/pdf_file/0011/294599/Factsheet-Toxoplasmosis-en.pdf.
2. Molan A, Nosaka K, Hunter M, Wang W. Global status of *Toxoplasma gondii* infection: systematic review and prevalence snapshots. *Trop Biomed* 2019; 36(4):898-925.
3. Mariani E, Polidori M, Cherubini A, Mecocci P. Oxidative stress in brain aging, neurodegenerative and vascular diseases: An overview. *Journal of Chromatography. B, Analytical Technologies in the Biomedical and Life Sciences* 2005; 827: 65–75.
4. Dincel G, Atmaca H. Role of oxidative stress in the pathophysiology of *Toxoplasma gondii* infection. *Int. J. Immunopathl Pharmacol* 2016; 29:226-240.
5. Da-Silva A, Munhoz T, Faria J, Vargas-Hernández G, Machado R, Almeida T et al. Increase nitric oxide and oxidative stress in dogs experimentally infected by *Ehrlichia canis*: effect on the pathogenesis of the disease. *Vet. Microbiol* 2013; 164(3-4):366-369.
6. Karaman U, Celik T, Kiran T, Colak C, Daldal N. Malondialdehyde, glutathione, and nitric oxide levels in *Toxoplasma gondii* seropositive patients. *Korean Journal of Parasitology* 2008; 46: 293–295.
7. Hatfield RH, and McKernan RM. CSF neuron-specific enolase as a quantitative

- marker of neuronal damage in a rat stroke model. *Brain Research* 1992; 577: 249–252.
8. Wei H, Wei S, Lindsay D, Pe H. A systematic review and meta-analysis of the efficacy of anti-Toxoplasma gondii medicines in humans. *PLoS One* 2015; 10: e0138204.
 9. Montazeri M, Sharif M, Sarvi S, Mehrzadi S, Ahmadpour E, Daryani A. A systematic review of in vitro and in vivo activities of anti-Toxoplasma drugs and compounds (2006–2016). *Front Microbiol* 2017 8: 25.
 10. Bernhoft A. A brief review on bioactive compounds in plants, In *Bioactive compounds in plants – benefits and risks for man and animals*, Oslo: *The Norwegian Academy of Science and Letters* 2010; 11–17.
 11. Shakya A. Medicinal plants: Future source of new drugs. *International journal of herbal medicine* 2016; 4(4):59–64.
 12. Gilani A, Rehman N, Mehmood M, Alkharfy K. Species differences in the antidiarrheal and antispasmodic activities of *Lepidium sativum* and insight into underlying mechanisms. *Phytother Res* 2013; 27: 1086–1094.
 13. Adamu M, Boonkaewwan C. Effect of *Lepidium sativum* L. (Garden Cress) seed and its extract on experimental *Eimeria tenella* infection in broiler chickens. *Kasetsart J (Nat Sci)* 2014; 48:28–37.
 14. Bahrami S, Razi Jalali M, Ramezani Z, Pourmehdi Boroujeni M, Toeimepour F. In vitro scolicidal effect of *Lepidium sativum* essential oil. *J Ardabil Univ Med Sci* 2016; 15: 395–403.
 15. Abuelenain G, Fahmy Z, Elshennawy A, Fahmy A, Ali E, Hammam O et al. The potency of *Lepidium sativum* and *Commiphora molmol* extracts on *Trichinella spiralis* stages and host interaction. *Adv Anim Vet Sci* 2021; 9 (9): 1376–1382.
 16. Youse H, Kazemian A, Sereshti M, Rahmanikhoh E, Ahmadiania E, Rafeian M, et al. Effect of *Echinophora platyloba*, *Stachys lavandulifolia*, and *Eucalyptus camaldulensis* plants on *Trichomonas vaginalis* growth in vitro. *Adv Biomed Res* 2012; 1.
 17. El-Moein N, Mahmoud E, Shalaby E. Antioxidant mechanism of active ingredients separated from *Eucalyptus globulus*. *Org Chem Curr Res* 2012; 1.
 18. Luís Â, Duarte A, Pereira L, Domingues F. Chemical profiling and evaluation of antioxidant and anti-microbial properties of selected commercial essential oils: a comparative study. *Medicine* 2017 4: 36.
 19. Juan M, Wenzel U, Ruiz-Gutierrez V, Daniel H, Planas J. Olive fruit extracts inhibit proliferation and induce apoptosis in HT29 human colon cancer cells. *J Nut* 2006; 136 (10):2553–7.
 20. Lee I, Kim D, Lee S, Kim K, Choi S, Hong J, et al. Triterpenoic acids of *Prunella vulgaris* var. *lilacina* and their cytotoxic activities in vitro. *Arch Pharm Res* 2008; 31 (12):1578–83.
 21. Jones J, Kruszon-Moran D, Wilson M, McQuillan G, Navin T, McAuley J. *Toxoplasma gondii* infection in the United States: seroprevalence and risk factors. *AmJ Epidemiol* 2001; 154 (4):357– 65.
 22. Kulkarni S, Canto C. The molecular targets of resveratrol. *Biochim Biophys Acta* 2015; 1852:1114–1123.
 23. Xia N, Daiber A, Forstermann U, Li H. Antioxidant effects of resveratrol in the cardiovascular system. *Br J Pharmacol* 2017; 174:1633–1646.
 24. de S´ a Coutinho D, Pacheco M, Frozza R, Bernardi A. Anti-Inflammatory effects of resveratrol: mechanistic insights. *Int J Mol Sci* 2018; 19: 1812.
 25. Contreras S, Ganuza A, Corvi M, Angel S. Resveratrol induces H3 and H4K16 deacetylation and H2A.X phosphorylation in *Toxoplasma gondii*. *BMC Research Notes* 2021; 141: 19.
 26. Szkudelska K, Okulicz M, Hertig I, Szkudelski T. Resveratrol ameliorates inflammatory and oxidative stress in type 2 diabetic Goto-Kakizaki rats, *Biomed. Pharmacother Biomed Pharmacother* 2020; 125: 110026.

27. Johnson L, Berggren K, Szaba F, Chen W, Smiley S. Fibrin-mediated protection against infection-stimulated immunopathology. *J Exp Med* 2003; 197: 801–806.
28. Köksal Z, Yanik K, Bilgin K, Yılmaz E Hokelek M. In Vivo Efficacy of Drugs against *Toxoplasma gondii* Combined with Immunomodulators. *Jpn. J Infect Dis* 2015; 69:113–117.
29. Bottari N, Baldissera M, Tonin A, Rech V, Alves C, D'Avila F et al. Synergistic effects of resveratrol (free and inclusion complex) and sulfamethoxazole-trimethoprim treatment on pathology, oxidant/antioxidant status, and behavior of mice infected with *Toxoplasma gondii*. *Microbial pathogenesis* 2016; 95:166–174.
30. Moore J, Yousef M, Tsiani E. Anticancer Effects of Rosemary (*Rosmarinus officinalis* L.) Extract and Rosemary Extract Polyphenols. *Nutrients* 2016; 8: 731.
31. Abdel Hamed E, Mostafa N, Fawzy E, Mohamed N, Ibrahim M, Rasha Attia R, et al . The delayed death-causing nature of *Rosmarinus officinalis* leaf extracts and their mixture within experimental chronic toxoplasmosis: Therapeutic and prophylactic implications. *Acta Tropica* 2021; 221: 105992.
32. Suvarna K, Christopher L, Bancroft J. *Bancroft's Theory and Practice of Histological Techniques, 7th Edition* 2013.
33. Hsu S, Raine L, Fanger H. A Comparative Study of the Peroxidase-anti peroxidase Method and an Avidin-Biotin Complex Method for Studying Polypeptide Hormones with Radioimmunoassay Antibodies, *American Journal of Clinical Pathology* 1981; 5(75): 734–738.
34. Hashish H, Kamal R. Effect of curcumin on the expression of Caspase-3 and Bcl-2 in the spleen of diabetic rats. *J Exp Clin Anat* 2015; 14: 18–23.
35. Mendez O, Koshy A. *Toxoplasma gondii*: Entry, association, and physiological influence on the central nervous system. *PLoS Pathog* 2017; 13- 7: e1006351.
36. Faucher B, Moreau J, Zaegel O, Franck J, Piarroux R. Failure of conventional treatment with pyrimethamine and sulfadiazine for secondary prophylaxis of cerebral toxoplasmosis in a patient with AIDS. *Antimicrob Chemother* 2011; 66 (7): 1654–1656.
37. Montazeri M, Mehrzadi S, Sharif M, Sarvi S, Tanzifi A, Aghayan S et al. Drug Resistance in *Toxoplasma gondii*. *Front Microbiol* 2018; 9:2587.
38. Ebrahimzadeh M, Taheri M, Ahmadpour E, Montazeri M, Sarvi S, Akbari M et al. Anti-toxoplasma effects of methanol extracts of *Feijoa sellowiana*, *Quercus castaneifolia*, and *Allium paradoxum*. *J Pharmacopuncture* 2017; 20: 220–226.
39. Mahmoudvand H, Sheibani V, Shojaee S, Mirbadie S, Keshavarz H, Esmaeelpour K et al. *Toxoplasma gondii* infection potentiates cognitive impairments of Alzheimer's disease in the BALB/c mice. *Journal of Parasitology* 2016; 102 (6):629-635.
40. Omar S. Oleuropein in olive and its pharmacological effects. *Sci Pharm* 2010; 78: 133-154.
41. Abugomaa A, Elbadawy M. Olive leaf extract modulates glycerol-induced kidney and liver damage in rats. *Environmental science and pollution research international* 2020; 27(17): 22100–22111.
42. Ren J, Chung S. “Anti-inflammatory effect of α -linolenic acid and its mode of action through the inhibition of nitric oxide production and inducible nitric oxide synthase gene expression via NF- κ B and mitogen-activated protein kinase pathways. *Journal of Agricultural and Food Chemistry* 2007; 13(55): 5073–5080.
43. Raish M, Ahmad A, Alkharfy K, Ahamad S, Mohsin K, Al-Jenoobi F et al. Hepatoprotective activity of *Lepidium sativum* seeds against D-galactosamine/lipopolysaccharide-induced hepatotoxicity in animal model. *BMC Complem Altern Med* 2016; 16: 501.
44. Al-Otaibi M, Al-Quraishy S, Al-Malki E, Abdel-Baki A. Therapeutic potential of the methanolic extract of *Lepidium sativum*

- seeds on mice infected with *Trypanosoma evansi*. *Saudi Journal of Biological Sciences* 2018; 1473–1477.
45. Balgoon M. Assessment of the Protective Effect of *Lepidium sativum* against Aluminum-Induced Liver and Kidney Effects in Albino Rat. *BioMed Research International* 2019; 4516730.
46. Mousa A, Elweza A, Elbaz H, Tahoun E, Shoghy K, Elsayed I. Eucalyptus Globulus protects against diclofenac sodium-induced hepatorenal and testicular toxicity in male rats. *Journal of Traditional and Complementary Medicine* 2020; 10: 521-528.
47. Mousavi P, Rahimi Esboei B, Pourhajibagher M, Fakhari M, Shahmoradi Z, Hejazi S et al. Anti-leishmanial effects of resveratrol and resveratrol nanoemulsion on *Leishmania major*. *BMC microbiology* 2022; 22(1): 56.
48. Highab S, Aliyu M, Muhammad B. Effect of Resveratrol on Liver Histopathology of Lead-induced Toxicity in Wistar Rats. *Journal of Pharmaceutical Research International* 2018; 20 (6): 1–8.
49. Liesenfeld O, Parvanova J, Zerrahn S, Han F, Heinrich M, Munoz F et al. The IFN γ -inducible GTPase, Irga6, protects mice against *Toxoplasma gondii* but not against *Plasmodium berghei* and some other intracellular pathogens. *PLoS One* 2011; 6: e20568.
50. Mccusker R, Kelley K. Immune-neural connections: How the immune system's response to infectious agents influences behavior. *Journal of Experimental Biology* 2013; 216: 84–98.

Cite as: Abd El Rahman, E., Nada, S., Ibrahim, N., Attia, R., Ibrahim, S., Salama, M. Anti-inflammatory and Anti-oxidative Effects of Some Medicinal Herbs on Chronic Murine Toxoplasmosis: A Histopathological and Immunohistochemical Study. *Afro-Egyptian Journal of Infectious and Endemic Diseases*, 2024; 14(1): 94-112. doi: 10.21608/aeji.2024.258749.1346